

S. Power · T. Casey · C. Folland · A. Colman · V. Mehta

## Inter-decadal modulation of the impact of ENSO on Australia

Received: 21 October 1998 / Accepted: 27 November 1998

**Abstract** The success of an ENSO-based statistical rainfall prediction scheme and the influence of ENSO on Australia are shown to vary in association with a coherent, inter-decadal oscillation in surface temperature over the Pacific Ocean. When this Inter-decadal Pacific Oscillation (IPO) raises temperatures in the tropical Pacific Ocean, there is no robust relationship between year-to-year Australian climate variations and ENSO. When the IPO lowers temperature in the same region, on the other hand, year-to-year ENSO variability is closely associated with year-to-year variability in rainfall, surface temperature, river flow and the domestic wheat crop yield. The contrast in ENSO's influence between the two phases of the IPO is quite remarkable. This highlights exciting new avenues for obtaining improved climate predictions.

### 1 Introduction

The El Niño-Southern Oscillation (ENSO) phenomenon affects climate over many parts of the world (Ropelewski and Halpert 1987; Philander 1990;

Halpert and Ropelewski 1992) including Australia (Nicholls 1985; Allan 1991). In fact the economic cost of Australian droughts often associated with ENSO is believed to run into hundreds of millions of dollars (Nicholls 1985, 1992). Managerial strategies based on ENSO forecasts could help to reduce this, with greater savings expected for more skilful forecasts (Adams et al. 1995).

ENSO and its teleconnections vary on inter-decadal time-scales (e.g. Wang and Ropelewski 1995; Allan et al. 1996; Wang and Wang 1996) and so one might expect that statistical prediction schemes based on ENSO would exhibit inter-decadal variability in their predictive capability. We will see in the following section that this is indeed the case. The cause of these variations is currently unknown. It is known, however, that a coherent pattern of surface temperature variability on inter-decadal time-scales over the Pacific Ocean (Latif et al. 1997; Folland et al. 1998; Zhang et al. 1997) is associated with fluctuations in both Australian rainfall (Latif et al. 1997; Folland et al. 1998; Kleeman et al. 1996; Power et al. 1998) and surface temperature (Power et al. 1998a) on the *same* long time scale. It therefore seems sensible to ask if there is any association between this Inter-decadal Pacific Oscillation (or IPO) and the inter-decadal variability in ENSO teleconnections with Australia.

To address these issues we will examine the inter-decadal variability in both the hindcast skill of an ENSO-based rainfall prediction scheme (Zhang and Casey 1992; Casey 1998) in Sect. 2 and the association between ENSO and Australian climate during different phases of the IPO in Sect. 3, using high-quality subsets of Australian rainfall (Lavery et al. 1992) and temperature (Torok and Nicholls 1996) records, a reconstruction of both the domestic wheat crop yield and of the flow rate of Australia's most important source of water for irrigation, the Murray River. The study concludes with a brief summary and discussion.

---

S. Power (✉)<sup>1,2</sup> · T. Casey

Bureau of Meteorology Research Centre, Melbourne, Australia  
<sup>1</sup>and the Cooperative Research Centre for Southern Hemisphere Meteorology, Monash University, Clayton, Victoria, Australia

Present address:

<sup>2</sup>National Climate Centre, Bureau of Meteorology,  
GPO Box 1289K Melbourne, VIC 3001, Australia  
E-mail: S. Power@bom.gov.au

C. Folland · A. Colman  
Hadley Centre for Climate Prediction and Research,  
Meteorological Office, Bracknell, Berkshire, UK

V. Mehta  
Joint Center for Earth System Science, University of Maryland/  
NASA Goddard Space Flight Center, MD, USA

## 2 Inter-decadal variation in rainfall prediction

A linear statistical scheme (Zhang and Casey 1992; Casey 1998) based on the Southern Oscillation Index (SOI, which measures ENSO variability) has been used to hindcast Australian rainfall anomalies for the period 1900–1997. The skill of the scheme is measured here by the score described by Potts et al. (1996), using a jack-knife, cross validation procedure (Wilks 1995). A “linear error in probability space” (LEPS) score is employed, which penalizes errors in terms of the distance between forecasts and observations in cumulative probability space. The scheme was applied every month during this period to “predict” (hindcast) rainfall anomalies for the following three month block. The skill in all one-degree squares east of 140°E were evaluated individually and then combined into a single average. The temporal evolution of this spatial average is presented in Fig. 1a. Note that in the long run guessing gives a zero score and that greater skill is indicated by a positive score.

Notice that the skill of the predictive scheme varies on all resolved time scales from inter-monthly to inter-decadal. It is possible that the inter-decadal variability of the skill score is simply random and that it has no connection with variability on a broader scale. On the other hand, as mentioned in the introduction, sea-surface temperature over the Pacific Ocean is associated with inter-decadal fluctuations in Australian climate, and so perhaps it also effects the predictive capability of the rainfall prediction scheme.

Various indices for this “inter-decadal Pacific Oscillation”, or **IPO**, derived from a variety of sources, are presented in Fig. 1b. All are derived from Empirical Orthogonal Function (EOF) analyses. The longest indices (from Folland et al. 1998) are derived from global data sets of seasonal sea-surface temperature (SST, solid bold line) and night-time marine air temperature (line with solid circles) back to 1856. In both cases the data were low pass filtered with a 13 year cut-off prior to performing the analysis. Annual totals are presented.

The shortest index (grey line) is derived from an EOF analysis of annual North Pacific SST data back to 1935 which had also been low pass filtered with an eight year cut-off (Mehta, personal communication). We then applied additional low pass filtering with a 13 year cut-off to be consistent with the other indices presented.

The third longest index (grey line with open circles) is derived from an EOF analysis of detrended monthly SST data over the extra-tropical North Pacific back to 1900 (Zhang et al. 1997; kindly provided by Dr Mantua NJ, University of Washington). We then calculated the annual totals of the time series of the first EOF and then low pass filtered the resulting time-series using a 13 year cut-off to produce the index depicted. See Power et al. (1998a) for further details on the filtering methodology. The index presented therefore represents

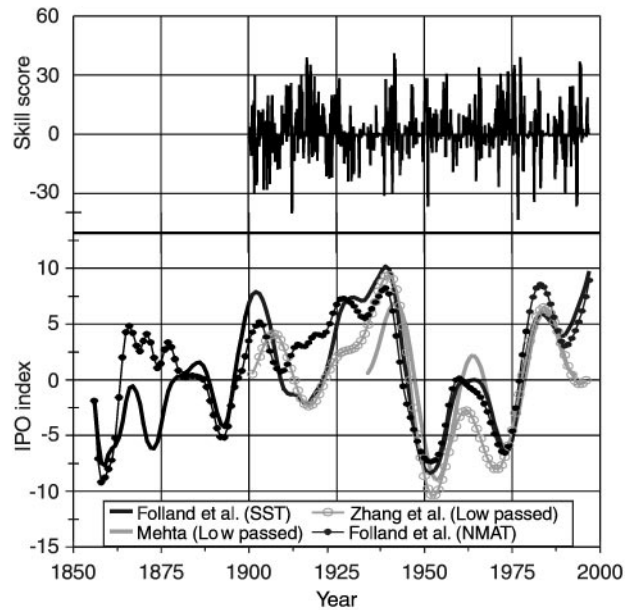


**Fig. 1 a** The temporal evolution of a skill score (Potts et al. 1996) averaged over eastern Australia for the rainfall prediction scheme (Zhang and Casey 1992; Casey 1998) from 1900 to 1997, using a jack-knife (Wilks 1995), cross validation procedure. The scheme was applied every month during this period to “predict” (hindcast) rainfall anomalies for the following three month block. **b** The temporal evolution of four indices of observed, coherent patterns of sea-surface temperature (SST) variability from various sources (Folland et al. 1998; Zhang et al. 1997; Mehta 1998) and one of night-time marine air temperature (Folland et al. 1998, labelled *NMAT*). The longest two time series (Folland et al. 1998) represent annual totals of seasonal records and are derived from EOF analyses of near-global data sets. The second shortest (based on a time-series calculated by Zhang et al. 1997, *grey line and circles*) was filtered using a low pass spectral filter with an 13 y cut-off (see Power et al. 1998a for further details on the filtering process), after combining monthly data into annual totals. It is derived from monthly SST data for the North Pacific. The shortest time series is based on an EOF analysis of annual SST data for the North Pacific (Mehta 1998). It has been multiplied by 15 to facilitate comparison. For the purposes of this study the amplitude is essentially arbitrary. The correlation coefficients between the indices depicted vary between 0.8 and 0.95. Further details given in the text.

the inter-decadal component of the variability evident in the original time series described by Zhang et al. (1997).

Note that this component has a time series which is similar to others calculated by Zhang et al. (1997) using SST from different regions (e.g. global). Mantua et al. (1997) also analyzed winter-time SST in the extratropical North Pacific and Northern Hemisphere surface and atmospheric variables. They referred to the coherent interannual to inter-decadal variability they saw in winter-time as the “Pacific Decadal Oscillation”, but noted that the variability was characterized by inter-decadal variability as it is here. Additionally, Zhang et al. (1997) showed that the temporal evolution of EOFs of SST from larger regions had an inter-decadal component which is very similar to the inter-decadal

component of the EOF of extra-tropical North Pacific SST. Furthermore, Folland et al. (1998) pointed out that their third EOF of low frequency SST has a very similar structure to the first EOF of low frequency, effectively detrended near-global SST calculated by Zhang et al. (1997). (The first EOF obtained by Folland et al. 1998 represents global warming, while the second represents out-of-phase temperature fluctuations between the Northern and Southern Hemispheres). This earlier work, together with the results presented here, suggest that the component of variability which occurs on inter-decadal time scales is common to all of the analyses described.

These results, combined with the fact that 10 year periods are not explicitly included in the low passed signals presented here, also leads us to prefer the term “*Inter-decadal Pacific Oscillation*” or IPO, to highlight the dominant time scale.

Despite the various differences in analysis and both the kind and geographical extent of the data used, the indices also bear a strong resemblance to each other (Folland et al. 1998; Power et al. 1998), with correlation coefficients varying between 0.8 and 0.95. This is especially true during the twentieth century when the data are more reliable. This increases confidence that they represent genuine climatic variability.

As mentioned already, the spatial structure of the various patterns, while not identical, are also very similar. A typical example is given in Fig. 2, which shows

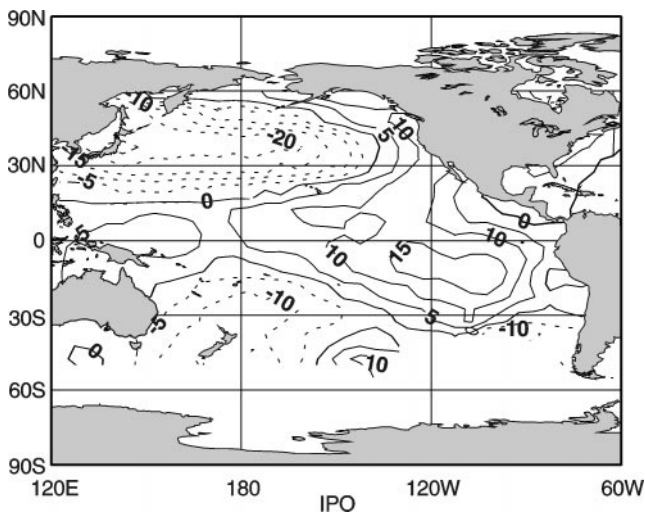


**Fig. 2** The SST signature of the IPO during its warm tropical Pacific phase (i.e. when the IPO Index is positive). This particular plot is based on an analysis of near-global SST data for 1911–1995 by Folland et al. (1998). Only the Pacific is shown here. It represents the third unrotated EOF of low frequency SST variability. A 13 y cut-off was used. It accounts for approximately 13% of the low frequency variability and 3% of the total variability (Folland et al.’s 1988 equivalent figure for the interannual El Niño mode is 16% of the total variability). The first EOF in the same analysis represents global warming, while the second represents out-of-phase temperature fluctuations between the Northern and Southern Hemispheres.

the structure when the IPO index is positive, when warm water in the tropical Pacific is flanked by cold water to the north and south. This plot is based on an EOF analysis of the global SST data for 1911–1995 (Folland et al. 1998), but its structure in the Pacific as shown here is reminiscent of an “*ENSO-like*” pattern (Zhang et al. 1997). Note that features outside the Pacific exist but these are generally smaller in amplitude.

To determine if the IPO is also associated with east Australian rainfall predictability on monthly to interannual time scales, the skill score was stratified according to the sign of the IPO index (derived from the time series calculated by Zhang et al. 1997) for magnitudes exceeding 0.05. This particular index is chosen here because it is the only one for which monthly data are available. In all subsequent calculations we use the longest available based on SST (Folland et al. 1998), as it is probably more reliable than the equally long index, based on air temperature, calculated by the same authors. The frequency distribution of the skill score (Fig. 3) shows that there are fewer negative scores (a negative score indicates poor performance), but more large positive scores (indicating increased skill) when the IPO index is negative. In fact the average score is significantly greater when the index is less than  $-0.05$  (average = 3.3) than when the index exceeds  $+0.05$  (average = 0.7 only). Thus when the IPO is negative, the seasonal predictability of Australian rainfall anomalies, based on a linear, lagged relationship with the SOI, tends to be significantly enhanced. The significance of this contrast was established at the 95% level by randomly selecting two distinct subsets from the original skill score time series 1000 times, and then

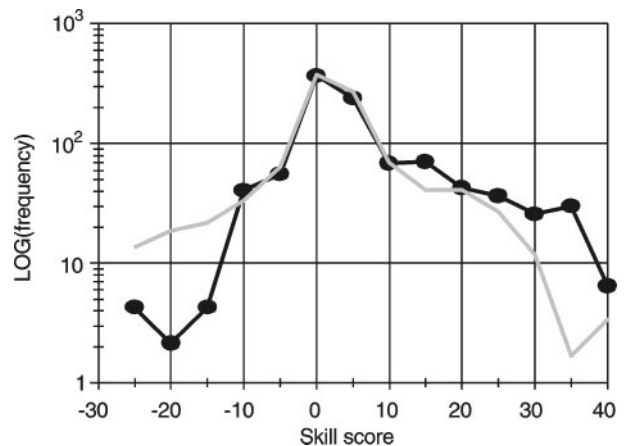


**Fig. 3** Frequency distribution of the skill score of the rainfall prediction scheme (Zhang and Casey 1992; Casey 1998) when the IPO (SST) index (Folland et al. 1998)  $< -0.05$  (line and circles) and  $> 0.05$  (line only). Thus when the IPO index  $< -0.05$  the frequency of both poor performance (negative skill scores) and low skill (small positive scores) is reduced and the frequency of skilful performance (high positive skill scores) is increased. Results are not especially sensitive to this choice of threshold (i.e. 0.05).

examining the frequency with which the difference in their average scores exceeded the corresponding figure for the bins (i.e. stratified IPO index) depicted in the figure.

### 3 Inter-decadal variation in the influence of ENSO on Australia generally

This suggests that the impact of ENSO on Australia may vary in association with the IPO. To test this we will examine the association between the SOI and various climate-related variables: rainfall, daily maximum temperature, river flow and an estimate of the domestic wheat crop yield. The rainfall and temperature were averaged over the entire continent (Power et al. 1998b). The river flow is a reconstruction of the natural Murray River flow rate at Albury, New South Wales. The record has had the effects of irrigation, land changes, etc., removed by taking diversions and reservoirs, for example, into account. The wheat crop yield is an estimate of the entire domestic wheat crop yield, and is based on a regression formula (Nicholls 1997) for the yield in terms of rainfall, and both daily minimum and maximum temperatures. It represents the yield relative to constant levels of technology, cultivar use and both crop extent and crop distribution. The rainfall, crop yield and river flow were all ranked prior to analysis to remove any potential ambiguity associated with skewed distributions. Values of the SOI were supplied by the Australian National Climate Centre representing normalized monthly anomalies of the difference between (un-normalized) Tahiti and Darwin mean sea-level pressure. All data were annually averaged.

**Table 1** The correlation coefficients between the SOI and important climate-related variables in Australia since 1910, stratified by the polarity of the IPO are tabulated. All of the coefficients in the second column headed “IPOI < -0.5” are significant at the 95% level except for the river flow-SOI coefficient which is only significant at the 90% level. None of the coefficients in the last column headed “IPOI > 0.5” are significant. IPOI refers to the IPO index. There are between 35 and 38 data elements in each bin. The low frequency part of the signals (i.e. periods greater than 13 y) were removed prior to analysis to avoid transferring energy from low to high frequencies by the binning procedure. The conclusions are unchanged if this preliminary step is omitted. A larger threshold of 0.5 is used here because we are dealing with annual rather than monthly totals. The results are not especially sensitive to this choice. The correlation coefficient for the SOI and maximum daily temperature is negative, consistent with simple 1-D models which relate surface temperature variability with cloud, rainfall, soil moisture and evaporative cooling (Power et al. 1998b).

Correlation coefficient between the SOI and	IPOI < -0.5	IPOI > +0.5
Rainfall	0.7	0.0
River flow	0.4	0.1
Temperature	-0.8	0.1
Crop yield	0.7	0.1

The correlation coefficients between the SOI and these important climate-related variables are presented in Table 1. The table indicates that the IPO does indeed modulate ENSO’s influence on Australia. Variations in rainfall, for example, are only significantly correlated with the SOI when the IPO index is negative. The contrast is really quite remarkable, with correlation coefficients of 0.7 during the negative phase but only 0.1 during the positive phase. This effect is not restricted to rainfall, it also extends to maximum surface temperature, river flow and the domestic wheat crop. Further illustration of the modulation is given in Fig. 4, which

**Fig. 4** The coloured lines represent correlation coefficients between the SOI and various Australian climate-related variables calculated in 13 y running blocks. The solid black line depicts the IPO (SST) Index (Folland et al. 1998). The correlations between temperature and the SOI have been multiplied by -1 to facilitate comparison. All series were high-pass filtered with a 13 y cut-off prior to calculating the correlation coefficients.

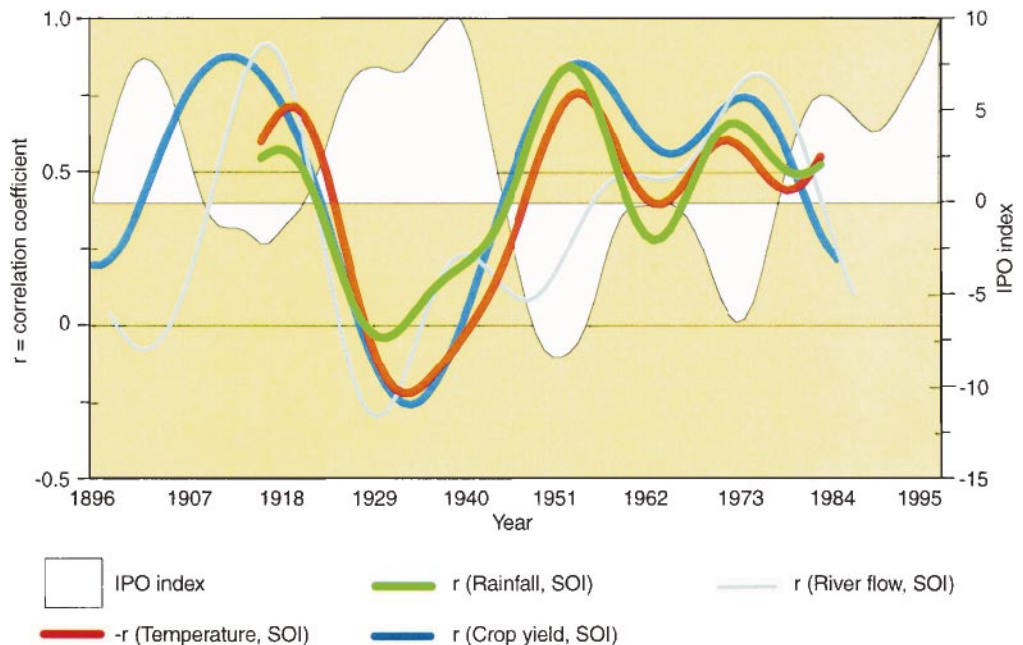


**Table 2** The variance of the Australian climate variables and the SOI calculated for years when the IPO (SST) index (Folland et al. 1998)  $< -0.5$  (N, negative) and then for years when the index  $> 0.5$  (P, positive). The ratio of these figures is presented in the second column marked “Total variance, N/P”. The ENSO contribution to the total variability in N and P was estimated by regressing the climate variable against the SOI, multiplying the SOI by the regression coefficient, and then calculating the variance of the resulting time series. There is an increase in variability in N relative to P for rainfall, temperature, the crop yield and the SOI. Periods greater than 13 y were again omitted prior to analysis. If this preliminary step is omitted the results are essentially the same, except that the ratio for river flow also exceeds unity. Results are based on records since 1910.

Climate variable	Total variance N/P	ENSO contribution N	ENSO contribution P
Rainfall	1.9	0.5	0.0
River flow	1.0	0.2	0.0
Temperature	1.9	0.6	0.0
Crop Yield	1.9	0.6	0.0
SOI	2.2	–	–

shows the IPO (SST) index along with time series of the correlation coefficients between the SOI and the various Australian climate-related variables in 13 year running blocks. The correlation coefficients between the IPO Index and the other curves are 0.8 (for the SOI-rainfall correlation coefficient time series),  $-0.8$  (SOI-temperature),  $-0.5$  (SOI-river flow) and  $-0.9$  (SOI-crop yield). There is also a tendency for the variability in both the ENSO and Australian climate to increase and for a larger fraction of the climate variability evident in Australia to be associated with ENSO when the IPO index is negative (Table 2).

#### 4 Discussion and summary

Here we have investigated inter-decadal variability in the influence of the El Niño – Southern Oscillation (ENSO) on Australia’s climate. This was done by examining the inter-decadal variability in both the performance of an ENSO-based rainfall prediction scheme and in the inter-relationships evident between year-to-year changes in both the Southern Oscillation Index (SOI) and Australian climate variables (rainfall, surface temperature, river flow and crop yield). A high quality subset of the available rainfall and temperature records was used. Both the performance of the prediction scheme and the association of Australian climate with ENSO vary on inter-decadal time scales. Part of this inter-decadal modulation occurs in association with an EOF of inter-decadal SST variability in the Pacific Ocean, which we refer to here as the IPO (Inter-decadal Pacific Oscillation). In fact when the IPO raises sea-surface temperatures (SSTs) in the tropical Pacific Ocean, there is no robust relationship between year-to-year Australian climate variations and ENSO, and

the prediction scheme performs poorly. On the other hand when the IPO reduces tropical Pacific SST the predictive scheme performs well and the association between ENSO and Australian climate is strong. Results presented here suggest that ENSO waxes and wanes on inter-decadal time-scales in association with the IPO. Whether or not this waxing and waning is an important influence outside Australia is currently under investigation.

A simple generalization of the rainfall prediction scheme to allow for different formulations depending on the phase of the IPO did not lead to a significant increase in overall hindcast skill. So it is not clear if the climate system is intrinsically less predictable during such periods or if predictive skill can be improved by utilizing knowledge of the IPO index more judiciously.

Note that some of the inter-decadal variability in the Pacific may arise from interactions between the atmosphere and ocean in the North Pacific (Latif and Barnett 1994) or perhaps as a response of the ocean to essentially stochastic atmospheric forcing (e.g. R. Saravanan, NCAR, personal communication). If theories of this kind are correct then part of the inter-decadal variability in the influence of ENSO on Australia seen here may be more than merely a statistical artifact of essentially random changes in individual ENSO events.

For example, the IPO is associated with fluctuations in rainfall (Latif et al. 1997; Power et al. 1998a) and temperature over Australia (Power et al. 1998a) on inter-decadal time-scales: when the central eastern Pacific is warm, eastern Australia exhibits a tendency to be warm and dry. This may modulate Australia’s response to ENSO forcing by modulating the underlying or background climatic conditions in Australia.

This is not the only possibility of course and so we are currently using models of the Earth’s climate to determine if the modulation arises because the IPO (1) directly modulates ENSO as suggested by Table 2, (2) affects the way ENSO variability in the tropics is communicated to Australia by modulating the state of the atmosphere through which the communication occurs, or (3) modulates Australia’s ability to cope with essentially unchanged ENSO forcing by modulating the background climatic conditions in Australia.

These issues take on added importance in light of the fact that the climate system may actually be in a state of low predictability, because the IPO index is near its most positive levels since the 1870’s. This may, in part, help to explain why rainfall predictions for Australia using statistically based models for 1997–1998 were not particularly successful.

We are also examining global data sets of rainfall and temperature to see if the modulation of ENSO’s influence by the IPO extends beyond Australia, and high quality, high resolution Australian data to see how these results depend upon season and location.

**Acknowledgements** We thank the Murray Darling Basin Commission for the river flow record, Australia's National Climate Centre for the Southern Oscillation Index, Dr. N. Mantua at the University of Washington for one of the EOF time series, Mr A. Kariko (BMRC) for the rainfall record and Dr N. Nicholls (BMRC) for the crop yield after 1950, derived earlier by C. Short at the Australian Bureau of Agriculture and Resource Economics.

## References

- Adams R, Bryant K, McCarl B, Legler D, O'Brien J, Solow A, Weiher R (1995) Value of improved long-range weather information. *Contemp Econ Pol*, 13: 10–19
- Allan RJ (1991) In: Teleconnections linking worldwide climate anomalies. Glantz, M. et al. (eds) Cambridge University Press. Cambridge, UK pp. 73–120
- Allan RJ, Lindesay J, Parker D (1996) El Nino Southern Oscillation and climatic variability. CSIRO Publishing, Collingwood, Australia, 402 pp
- Casey TM (1998) Assessment of a seasonal forecast model. *Aust Meteorol Mag* 47: 102–112
- Folland CK, Parker DE, Colman AW, Washington R. (1998) Large-scale modes of ocean surface temperature since the late nineteenth century. Hadley Centre, UK Meteorological Office, Clim Res Tech Note, CRTN 81, 45 pp
- Halpert MS, Ropelewski CF (1992) Surface temperature patterns associated with the Southern Oscillation. *J Clim* 5: 577–593
- Kleeman R, Colman RA, Smith NR, Power SB (1996) A recent change in the mean state of the Pacific basin climate. *J Geophys Res (Oceans)*, 101: 20 483–20 499
- Latif M, Barnett TP (1994) Causes of decadal climate variability over the North Pacific and North America. *Science* 266: 634–637
- Latif M, Kleeman R, Eckert C (1997) Greenhouse warming, decadal climate variability, or El Niño? An attempt to understand the anomalous 1990 s. *J Clim* 10: 2221–2239
- Lavery B, Kariko A, Nicholls N (1992) An historical rainfall data set for Australia. *Aust Meteorol Mag* 40: 33–39
- Mantua NJ, Hare SR, Zhang Y, Wallace JM, Francis RC (1997) A Pacific interdecadal climate oscillation with impacts on salmon production. *Bull Am Meteorol Soc* 78: 1069–1079
- Nicholls N (1985) Towards the prediction of major Australian droughts. *J Climatol* 5: 553–560
- Nicholls N (1992) Historical El Niño/Southern Oscillation variability in the Australian region. In: Diaz HF, Margraf V (eds) *El Niño, historical and paleoclimatic aspects of the Southern Oscillation*. Cambridge University Press, Cambridge, UK, pp 151–174
- Nicholls N (1997) Increased Australian wheat yield due to recent climate trends. *Nature* 387: 484–485
- Philander SG (1990) *El Niño, La Niña and the Southern Oscillation*. International Geophysical Series, 46, Academic Press, 293 pp
- Potts JM, Folland CK, Jolliffe IT, Sexton D (1996) Revised “LEPS” scores for assessing climate model simulations and long-range forecasts. *J Clim*, 9: 34–53
- Power S, Tseitkin F, Mehta V, Lavery B, Torok S, Holbrook, N (1998a) Decadal climate variability in Australia during the twentieth century. *Int J Climatol*, (accepted)
- Power S, Tseitkin F, Torok S, Lavery B, Dahni R, McAvaney B (1998b) Australian temperature, Australian rainfall and the Southern Oscillation Index, 1910–1992: coherent variability and recent changes. *Aust Meteorol Mag* 47: 85–101
- Ropelewski CF, Halpert MS (1987) Precipitation patterns associated with the high index phase of the Southern Oscillation. *J Clim* 115: 1606–1626
- Torok S, Nicholls N (1996) A historical annual temperature data set for Australia. *Aust Meteorol Mag* 45: 251–260
- Wang B, Wang Y (1996) Temporal structure of the Southern Oscillation as revealed by waveform and wavelet analysis. *J Clim* 9: 1586–1598
- Wang XL, Ropelewski CF (1995) An assessment of ENSO-scale secular variability. *J Clim* 8: 1584–1599
- Wilks DS (1995) *Statistical methods in the atmospheric sciences: an introduction*. Academic Press, 467 pp
- Zhang X-G, Casey TM (1992) Long-term variations in the Southern Oscillation and relationships with Australian rainfall. *Aust Meteorol Mag* 40: 211–225
- Zhang Y, Wallace JM, Battisti DS (1997) ENSO-like interdecadal variability: 1900–93. *J Clim* 10: 1004–1020